An Allosteric Mechanism Controls Antigen Presentation by the H-2K^b Complex†

Dmitry M. Gakamsky,*,‡ Lisa F. Boyd,§ David H. Margulies,§ Daniel M. Davis,|| Jack L. Strominger,|| and Israel Pecht‡

Department of Immunology, The Weizmann Institute of Science, Rehovot 76100, Israel, Molecular Biology Section, National Institute of Allergy and Infectious Diseases, National Institutes of Health, Bethesda, Maryland 20892-1892, and Department of Molecular and Cellular Biology, Harvard University, 7 Divinity Avenue, Cambridge, Massachusetts 02138

Received March 12, 1999; Revised Manuscript Received May 26, 1999

ABSTRACT: The mechanism of assembly/dissociation of a recombinant water-soluble class I major histocompatibility complex (MHC) H-2K^b molecule was studied by a real-time fluorescence resonance energy transfer method. Like the H-2K^d ternary complex [Gakamsky et al. (1996) *Biochemistry 35*, 14841−14848], the interactions among the heavy chain, β_2-microglobulin (β_2m), and antigenic peptides were found to be controlled by an allosteric mechanism. Association of the heavy chain with β_2m increased peptide binding rate constants by more than 2 orders of magnitude and enhanced affinity of the heavy-chain molecule for peptides. Interaction of peptides with the heavy-chain binding site, in turn, increased markedly the affinity of the heavy chain for β_2m. Binding of peptide variants of the ovalbumin sequence (257−264) to the heavy chain/β_2m heterodimer was found to be a biphasic reaction. The fast phase was a second-order process with nearly the same rate constants as those of binding of peptides derived from the influenza virus nucleoprotein 147−155 to the H-2K^d heavy chain/β_2m heterodimer [$(3.0 \pm 1.0) \times 10^{-6}$ M^{-1} s^{-1} at 37 °C]. The slow phase was a result of both the ternary complex assembly from the "free" heavy chain, β_2m, and peptide as well as an intramolecular conformational transition within the heavy chain/β_2m heterodimer to a peptide binding conformation. Biexponential kinetics of peptide or β_2m dissociation from the ternary complex were observed. They suggest that it can exist in two conformations. The rate constants of β_2m dissociation from the H-2K^b ternary complex were, in the limits of experimental accuracy, independent of the structure of the bound peptide, though their affinities differed by an order of magnitude. Dissociation of peptides from the K^b heavy chain was always faster than from the ternary complexes, yet the heavy chain/peptide complexes were considerably more stable compared with their K^d/nucleoprotein peptide counterparts.

Recognition by T-cell receptors (TCRs)[1] of class I major histocompatibility complex (MHC-I) encoded molecules carrying an antigenic peptide is the initial event in the cascade of the cytotoxic immune response. Cell response to the TCR−ligand interactions depends on the number and structure of MHC/peptide complexes as well as their affinity for the TCR. Although significant progress has been gained in elucidating the peptide binding motifs of MHC-I-encoded molecules (*2*, *3*), the quantitative characterization the MHC-I heavy chain−β_2m−peptide interactions is still limited (*4*−*9*). Early studies indicated an important role for β_2m in cooperative peptide/MHC interactions and in determining the conformation of the ternary complex (*10*−*14*). More recent studies have pursued the contribution of peptide and β_2m to the stability of the MHC-I ternary complexes, both on cell surfaces and of the isolated molecules investigated in vitro (*15*−*17*). Our earlier study of H-2K^d−peptide complexes established a key role for β_2m in modulating the heavy-chain binding site affinity for peptides (*1*). Although "free" H-2K^d heavy chain could bind peptides, such complexes dissociate within seconds (unpublished results). Association of the heavy chain with β_2m significantly slowed peptide dissociation. Dissociation time constants of the studied peptide series, based on the sequence of influenza virus nucleoprotein (147−155), were in the range of 2−40 min (37 °C), depending on peptide structure. Heavy-chain association with β_2m altered the heavy-chain peptide binding conformation, yielding peptide affinities in the nano- or subnanomolar range at 20 °C. Although the H-2K^d heavy chain/β_2m heterodimer is unstable and dissociates within several minutes at physiological temperature, bound peptides, even of the lowest affinity, slowed β_2m dissociation (unpublished results). Peptide dissociation lowered the affinity of the heterodimer and led to β_2m dissociation. The heavy chain, in turn, lost its high peptide binding affinity upon β_2m dissociation. These allosteric affinity modulations are most likely related to structural changes that occur in the heavy chain upon interaction with β_2m and peptides. The appearance and decay of specific epitopes on MHC-I molecules resulting from peptide and β_2m interactions (*11*, *19*−*21*) are characteristics

† This study was supported by the European Community, Grant BIOTECH (B104-CT96-0135), Life Sciences and Technologies Biotechnology Program (1994−1998), and by the John Hopkins University−Weizmann Institute cooperative research program.

* Corresponding author: Phone 972-8-9342551; Fax 972-8-9344141; E-mail lidima@wis.weizmann.ac.il.

‡ The Weizmann Institute of Science.

§ NIAID.

|| Harvard University.

[1] Abbreviations: TCR, T-cell receptor; MHC-I, class I major histocompatibility complex; **hc**, heavy chain; OVA, ovalbumin; **p**, peptide; β_2m, β_2-microglobulin; APC, antigen presenting cell; dansyl aziridine, 5-(dimethylamino)naphthalene-1-sulfonyl aziridine; TR, Texas red.

10.1021/bi9905821 CCC: $18.00
Published on Web 08/24/1999

consistent with such an allosteric mechanism. These cooperative interactions among the H-2K^d ternary complex components make its dissociation on the cell surface irreversible, thereby minimizing the reloading with exogenous peptides (*1*). These earlier observations raised the question to what extent such allosteric interactions are general features of different class I alleles. Here we present results of studies of the thermodynamics and kinetics of the interactions of another mouse class I molecule, H-2K^b, with β_2m and different peptides. The results provide independent support for the operation of allosteric interactions among components of another MHC-I molecule and thus support viewing this as a general mechanism of MHC-I−peptide interaction.

MATERIALS AND METHODS

Peptides. Unless otherwise stated, all chemicals were purchased from Sigma and were of highest purity available. Dansyl aziridine [5-(dimethylamino)naphthalene-1-sulfonyl aziridine] and Texas Red C_2 maleimide (TR) were purchased from Molecular Probes (*22*). The single-site mutation of the human β_2m with serine 88 replaced by cysteine and its labeling with TR were performed as described (*23*). Ovalbumin peptide SIINFEKL (OVA, residues 257−264) and a series of its cysteine-substituted variants, OVA3C (SI**C**NFEKL), OVA4C (SII**C**FEKL), OVA6C (SIINF**C**KL), and OVA7C (SIINFE**C**L), were synthesized by automated solid-phase methodology on an Applied Biosystems Model 432A synthesizer with the manufacturer's standard Fmoc protocol. The substituted cysteines in the variant peptides were dansylated to yield the respective derivatives as follows: 0.3 mL (10-fold molar excess) of dansyl aziridine in dimethylformamide was added to 1 mL of peptide solution (3 mg/mL) in 0.1 M bicarbonate buffer, pH = 8.2, and allowed to react for 2 h at room temperature in the dark. Labeled peptides were purified by HPLC. Concentrations of non-dansylated peptides and proteins were determined spectrophotometrically by using the extinction coefficients 5.60×10^3 M^{-1} cm^{-1} at 280 nm for tryptophan, 1.42×10^3 M^{-1} cm^{-1} at 274 nm for tyrosine, and 1.97×10^2 M^{-1} cm^{-1} at 257 nm for phenylalanine (*24*). Concentrations of dansylated peptides were determined by using the extinction coefficient 4.57×10^3 M^{-1} cm^{-1} at 335 nm of dansyl (*25*).

The above variants of peptides comprising residues 257−264 of ovalbumin were synthesized with cysteine substitution at positions that do not interfere with the peptide binding motif to H-2K^b (*26*−*28*).

Preparation of "Empty" H-2K^b Molecules and Purification of the Heterodimer. The soluble murine class I MHC H-2K^b molecule was produced in a transfected L cell line and purified by immune affinity chromatography as described previously (*29*). Then, the complex was gel-filtered on a Superose 12 column equilibrated with 8 M urea, 20 mM Tris, and 150 mM NaCl buffer, pH 7.5. This procedure released any bound peptide that copurified with the H-2K^b. The collected fractions of the heavy chain and β_2m were transferred to dialysis tubes with a 6 kDa cutoff and dialyzed overnight at 4 °C, either separately or together against the same buffer without urea. Samples of the heavy chain/β_2m heterodimer were concentrated to 14 μM and stored at 4 °C. Samples of "free" heavy chains were concentrated to ≤1 μM and used immediately for the binding assays.

Extinction coefficients of H-2K^b/β_2m and β_2m molecules were calculated as 9.2×10^4 M^{-1} cm^{-1} and 2.1×10^4 M^{-1} cm^{-1} at 280 nm, respectively, based on the extinction coefficients of tryptophan and tyrosine (*24*).

Throughout these studies, human β_2m was employed instead of its mouse counterpart because of the obtained higher yields of H-2K^b/human β_2m heterodimers compared to those with the mouse β_2m.

Fluorescence Binding Assays. Titrations and interaction kinetics measurements were carried out on a PTI spectrofluorometer with a single photon counting registration system. The sample holder's temperature was controlled to ±0.5 °C. The experiments were carried out in a 4 × 4 mm magnetically stirred, quartz optical cuvette. An excitation wavelength of 290 nm (slit width 4 nm) and an emission wavelength of 530 nm (slit width 16 nm) were used. All experiments were carried out in 20 mM Tris buffer, pH 7.5.

Peptide affinity and the kinetics of the ternary complex formation and decay were investigated by monitoring of the nonradiative energy transfer from intrinsic H-2K^b tryptophans to the dansyl conjugated to the bound peptides at the indicated positions. This provided direct monitoring of the reaction time course. Different sites of dansyl chromophore conjugation to the peptide analogues yielded distinct degrees of energy transfer. The best energy transfer efficiency was observed when the chromophore was attached to the third amino acid from the N-terminus. This indicates that tryptophans 51, 60, and 67 of H-2K^b contribute most of the energy transfer to the dansyl. Therefore, accuracy of equilibrium titrations or kinetic curves was highest for the OVA3C-DNS peptide. Peptide binding kinetics were studied after dilution of a small aliquot (1−3 μL) of one solution (usually 14 μM heterodimer stock) into 140 μL of the other (usually peptide) by a micrometric pipet (Eppendorf). Peptide exchange from the ternary complex was monitored by the addition of 40−50-fold excess unlabeled OVA peptide, which is assumed to block the rebinding of the dissociated labeled peptide.

Peptide binding/dissociation kinetic data were processed by a program that provides a nonlinear fit to an arbitrary model, which in our case was a sum of exponential components ($i = 1-4$) with a background: $y(t) = \alpha_0 + \sum\alpha_i \exp(-t/\tau_i)$.

RESULTS

We have previously studied the interactions of peptides derived from the influenza virus nucleoprotein peptide with the mouse MHC-I molecule H-2K^d in its water-soluble form and observed a marked cooperativity in the interactions between the heavy chain, peptide, and β_2m. To extend these findings and determine whether this cooperativity is a general feature of all class I MHC molecules, we selected H-2K^b, a molecule for which a high-resolution three-dimensional structure has been determined crystallographically in its complexes with four different peptides (*31*−*34*), including the ovalbumin peptide 257−264. Since we intended to monitor peptide interaction by fluorescence resonance energy transfer, we employed several synthetic peptides that were covalently labeled by a dansyl at cysteine residues. As expected from the 3D structure (pdb code 1VAC), such

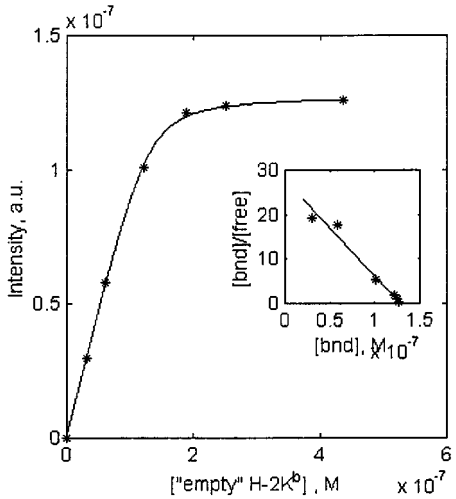

FIGURE 1: Example of an equilibrium titration experiment. Six aliquots of H-2K^b/β_2m heterodimer stock solution were added to 145 mL of OVA3C-DNS solution (0.13 μM) in 20 mM Tris NaCl buffer, pH = 7.5 at 25 °C. Fluorescence of the dansyl group was monitored at 530 nm via nonradiative energy transfer from intrinsic tryptophans of the H-2K^b heavy chain excited at 280 nm. The fluorescence intensity values were corrected for the sample dilution. Scatchard analysis of the binding curve is shown in the inset. The equilibrium dissociation constant of peptide OVA3C-DNS from the H-2K^b/β_2m heterodimer was calculated as 4.6 ± 2.0 nM.

modifications at the $N + 4$ and $N + 7$ positions of the 257−264 OVA sequence did not affect the peptide−MHC interactions, whereas at the $N + 3$ position it caused a reduction in peptide affinity.

Equilibrium Titrations. Equilibrium titrations of the H-2K^b/β_2m heterodimer were carried out with OVA3C-DNS and OVA7C-DNS. A typical saturation binding curve calculated from an equilibrium titration of OVA3C-DNS (0.13 μM) with H-2K^b/β_2m heterodimer at 25 °C is shown in Figure 1. The equilibrium dissociation constant, K_d, was calculated from the Scatchard analysis (inset). The equilibrium dissociation constants were 4.6 ± 2.0 nM for OVA3C-DNS and 0.5 ± 0.2 nM for OVA7C-DNS.

Peptide Binding to the H-2K^b/β_2m Heterodimer Is Biphasic. Typical curves of peptide binding time courses recorded under pseudo-first-order conditions at 20 °C are shown in Figure 2. The time course of the reaction was always biphasic. The amplitudes of the fast phase were found to depend on the employed experimental protocol. For example, a maximum amplitude was observed when a small aliquot (3 μL) of a 14 μM stock H-2K^b/β_2m heterodimer solution was added to the peptide solution (145 μL, 0.45 μM). However, when the same aliquot of the heterodimer was first diluted, and the peptide was added with a time delay, the amplitude of the fast phase declined as a function of that delay. The amplitude α_1 of the fast exponential term of the peptide binding kinetics, evaluated from a biexponential analysis [$y(t) = \alpha_0 - \alpha_1 \exp(-t/\tau_1) - \alpha_2 \exp(-t/\tau_2)$] are shown in the inset to Figure 2. The amplitude of the fast binding phase decayed biexponentially with the fast decay time constant of 4 ± 2 min and the slow one longer than 20 min. This biphasic dissociation of the heterodimer suggests that it has two conformations.

To further pursue the mechanism underlying the two phases observed in peptide binding, the time course was recorded at 0 °C and at different OVA6C-DNS peptide

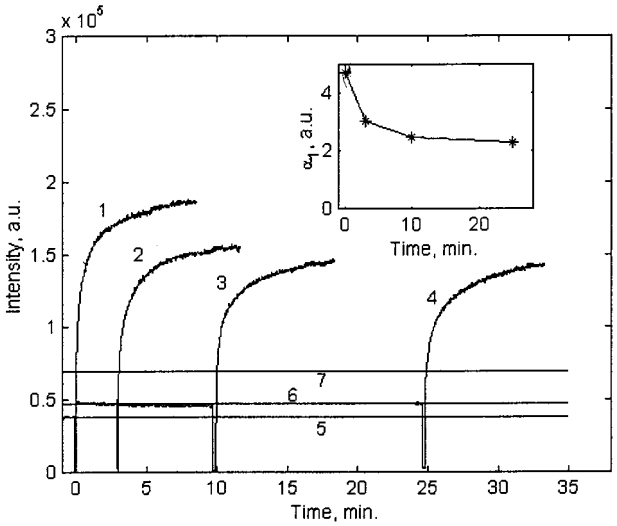

FIGURE 2: Time courses of OVA7C-DNS binding to H-2K^b heavy chain/β_2m heterodimer. A small aliquot (3 μL) of a 17.5 μM stock heterodimer solution was added to peptide solution (148 μL, 0.45 μM) (curve 1). Time courses (curves 2−4) were recorded for the same concentrations but the heterodimer was first diluted 50-fold from stock solution, and peptide was added to the solution with time delays of 3, 10, and 25 min, respectively. The fluorescence intensity changes were monitored at 530 nm upon 280 nm excitation at 20 °C. Lines 5 and 6 show fluorescence signals from the solution containing either peptide or heterodimer, respectively. Line 7 shows the fluorescence intensity level from which the signal has increased due to the fluorescence energy transfer. The amplitudes of the fast exponential term, α_1, were evaluated from a biexponential analysis of the reaction curves by the formula $y(t) = \alpha_0 - \alpha_1 \exp(-t/\tau_1) - \alpha_2 \exp(-t/\tau_2)$ and are shown in inset.

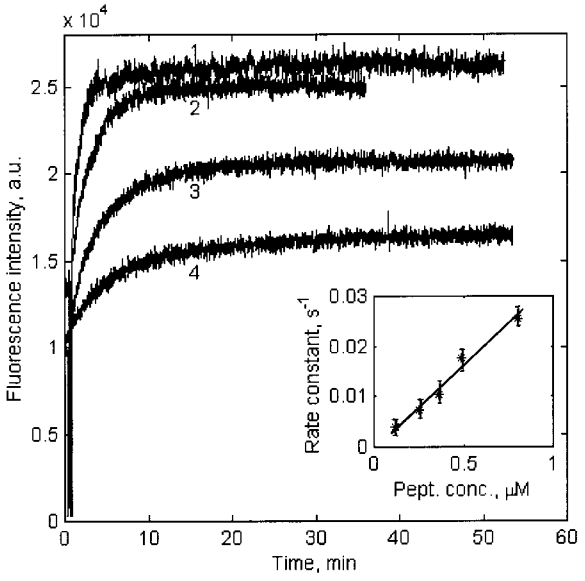

FIGURE 3: Time courses of OVA6C-DNS binding to H-2K^b heavy chain/β_2m heterodimer at 0 °C: [heterodimer] = 0.06 μM, [OVA6C-DNS] = 0.75 (1), 0.5 (2), 0.25 (3), and 0.125 μM (4). (Inset) Concentration dependence of the rate constants of the fast binding phase as a function of peptide concentration.

concentrations as illustrated in Figure 3. Curves 1−4 correspond to peptide concentrations of 0.8, 0.5, 0.25, and 0.125 μM, respectively, and 0.06 μM heterodimer concentration. Results of the biexponential analysis of the experimental time courses are listed in Table 1. The rate constant of the fast binding phase was found to be a linear function of peptide concentration (Figure 3, inset). The amplitude of this

Table 1: Results of an Analysis of OVA6C-DNS Binding Kinetics to "Empty" H-2K^{b} [a]

[OVA6C-DNS] (μM)	α_1	τ_1 (s)	k_1 ($\times 10^4$ M^{-1} s^{-1})	α_2	τ_2 ($\times 10^3$ s)	k_2 ($\times 10^{-4}$ s^{-1})
0.12	0.39 ± 0.05	247 ± 50	3.4 ± 0.9	0.61 ± 0.05	3.7 ± 21.5	2.7 ± 2.0
0.25	0.37± 0.05	135 ± 25	3.0 ± 0.4	0.63 ± 0.05	4.4 ± 1.5	4.4 ± 2.0
0.37	0.31± 0.05	96 ± 25	2.8 ± 0.7	0.69 ± 0.05	1.5 ± 1.2	6.5 ± 2.0
0.49	0.64± 0.05	57 ± 12	3.6 ± 1.0	0.36 ± 0.05	3.4 ± 1.5	3.0 ± 2.0
0.80	0.64± 0.05	39 ± 10	3.9 ± 1.0	0.36 ± 0.05	2.2 ± 1.5	4.5 ± 2.5

[a] Biexponential model: $y(t) = 1 - \alpha_1 \exp(-t/\tau_1) - \alpha_2 \exp(-t/\tau_2)$. $t = 0$ °C. ["Empty" H-2K^{b}] = 0.05 μM.

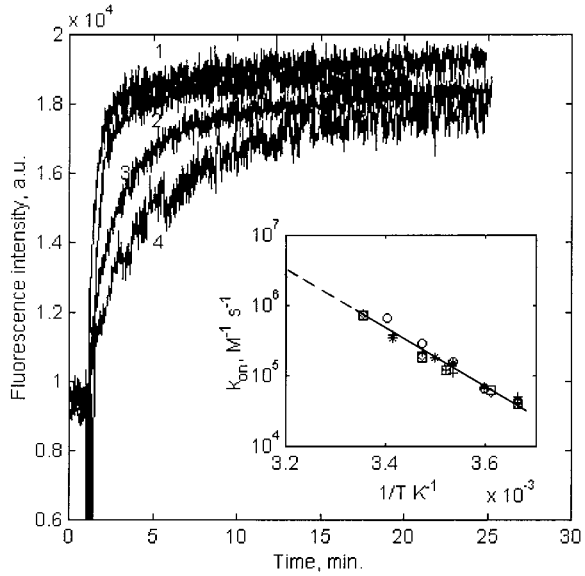

FIGURE 4: Temperature dependence of OVA6C-DNS (0.25 μM) binding time course to H-2K^{b} heavy chain/β_2m heterodimer (0.06 μM). t = 15 (1), 10 (2), 5 (3), and 0 °C (4). (Inset) Arrhenius plots of peptide binding rate constants of OVA6C-DNS (*), OVA3C-DNS (□) and OVA7C-DNS (◇) to H-2K^{b} heavy chain/β_2m and dNP19 (○) and dNP22 (+) to H-2K^{d} heavy chain/β_2m heterodimers. The peptide binding rate constant at 37 °C was calculated by extrapolation to be (3.0 ± 1.0) × 10^6 M^{-1} s^{-1}.

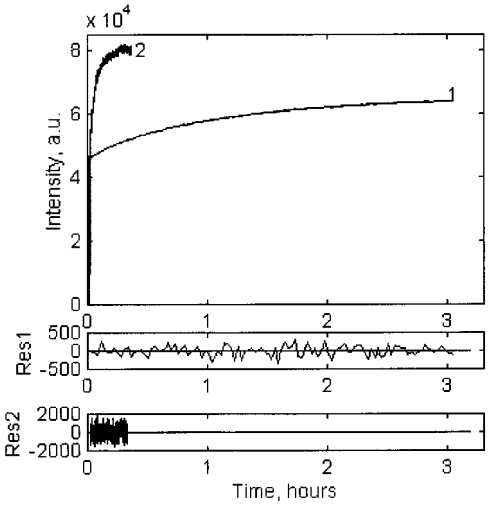

FIGURE 5: Time courses of OVA7C-DNS (1 μM) binding to "free" H-2K^{b} heavy chain (0.1 mM), (t = 3700 ± 500 s) alone (curve 1) and in the presence of β_2m (0.25 mM) (α_1 = 0.36, τ_1 = 100 ± 20 s; α_2 = 0.64, and τ_2 = 470 ± 80 s (curve 2) at 10 °C.

phase decayed in parallel to the slowing down of the reaction rate, caused by lowering of the peptide concentration.

The fast phase of peptide binding reaction to the H-2K^{b}/β_2m heterodimer exhibited a linear temperature dependence, as shown in the Arrhenius plot over the 0−15 °C range (Figure 4, inset). The peptide binding kinetics at physiological temperature were too fast to be resolved by the experimental protocol employed and the rate constants were calculated by extrapolation to 37 °C, yielding k_{on} = (3.0 ± 1.0) × 10^6 M^{-1} s^{-1}.

Assembly of the Ternary Complex from Heavy Chain, β_2m, and Peptide. No simple concentration dependence of the slow peptide binding phase was revealed in experiments such as that illustrated by Figure 2. To assign this slow phase to a specific step of the reaction, interactions between the "free" heavy chain, β_2m, and peptides were studied under different experimental conditions at 20 °C. When the reaction was initiated by dilution of a small aliquot of the heavy chain/β_2m heterodimer stock solution (final concentration 0.2 μM) into a solution of OVA3C-DNS (2 μM) without or with human β_2m (9.4 μM), the reaction time courses were nearly identical (α_1 = 0.4, τ_1 = 9 s, α_2 = 0.6, and τ_2 = 79 s without human β_2m vs α_1 = 0.5, τ_1 = 6 s, α_2 = 0.5, and τ_2 = 70 s with human β_2m), indicating that under these experimental conditions the slow phase was due to a monomolecular process within the heterodimer. However, at lower concentrations of the heterodimer and peptide, the reaction rate depended on the concentrations of both reagents.

We further studied this reaction by mixing "free" heavy chain with peptide with or without addition of β_2m. Interaction of the "free" heavy chain with peptides is illustrated by Figure 5, curve 1. The time course of OVA7C-DNS (1 μM) binding to the "free" heavy chain (0.1 μM) was found to be nearly exponential (Figure 5, curve 1) and about 2000-fold slower than that of its binding to the H-2K^{b}/β_2m heterodimer. The reaction rate constants depended linearly on peptide concentration (see Figure 6A and Table 2). Addition of β_2m (final concentration 0.25 μM) to the above sample (Figure 5, curve 1) significantly accelerated the reaction time course (Figure 5, curve 2). Peptide binding to the heavy chain was an activation-dependent process as shown by its temperature dependence in the Arrhenius coordinates plotted in Figure 6B. The activation energy of this process was found to be 5.5 ± 2.0 kcal M^{-1}.

The ternary complex assembly from "free" heavy chains (0.1 μM), β_2m (0.42 μM), and OVA7C-DNS (0.88 μM) at 10 °C is shown in Figure 7 curve 1. The time courses of the ternary complex assembly from three subunits was studied with different β_2m concentrations and experimental protocols and was found to be a multiexponential one. Therefore two- or three-exponential fits were attempted in the analysis of the experimental results. When heavy chain, β_2m, and peptide were mixed at the same time (curve 1), the time course of ternary complex formation fit well to a biexponential function. The fast phase was concentration-dependent while the slow one was not. Results of the double-exponential analysis of the assembly process are listed in Table 3. Preincubation of the heavy chain and β_2m stock solutions

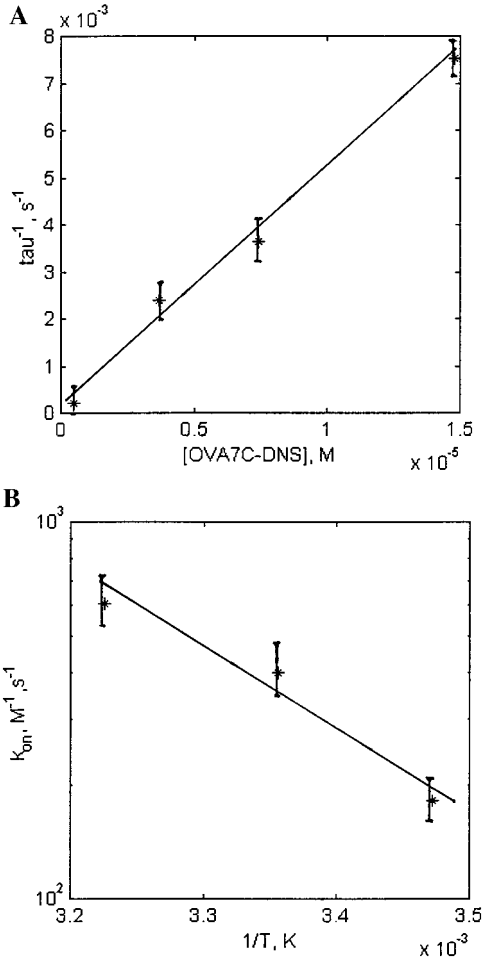

FIGURE 6: (A) Reaction rate constants of OVA7C-DNS binding to H-2K^b heavy chain at 25 °C plotted as a function of peptide concentration. (B). Arrhenius plot of peptide binding rate constants to H-2K^b heavy chain. Activation energy is about 5.5 ± 1.0 kcal M^{-1}.

Table 2: Results of an Analysis of OVA7C-DNS Binding Kinetics to H-2K^b Heavy Chain[a]

[OVA7C-DNS] (mM)	τ_1 (s)	k (M^{-1} s^{-1})
0.5	4800 ± 600	415 ± 60
3.7	420 ± 40	640 ± 70
7.4	274 ± 30	490 ± 50
14.8	133 ± 15	508 ± 50

[a] Exponential model; t = 0 °C, ["empty" H-2K^b] = 0.05 μM.

for 1 h at 4 °C prior to dilution into the peptide solution (to a final concentration identical to that of the above experiment) (curve 1, Figure 7) increased the amplitude of the fast phase due to the appearance of an additional component with the highest rate constant. The new phase was due to peptide binding to the newly formed heavy chain/β_2m heterodimers (curve 2, Figure 7).

Dissociation of β_2m and Peptides from the Heavy Chain or Ternary Complex. The interaction of the β_2m and the mouse H-2K^b heavy chain was also studied by using a TR-labeled C88S mutant of human β_2m. It was found earlier (*35*) that such a labeling of the β_2m mutant causes its oligomerization, which significantly quenches the TR fluorescence. The oligomers dissociate upon interaction with heavy chains, causing TR fluorescence intensity to increase. These fluorescence changes were used to directly measure

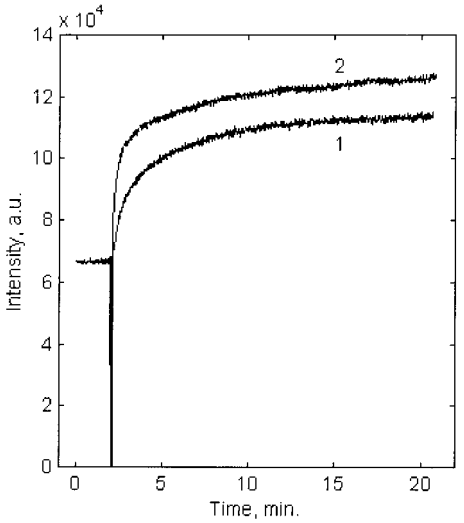

FIGURE 7: Assembly of the H-2K^b ternary complex from separated heavy chain (0.1 μM), β_2m (0.42 μM), and OVA7C-DNS (0.88 μM) at 25 °C. Reaction was initiated by simultaneous mixing of the heavy chain, β_2m, and peptide (1) or by dilution of solutions preincubated at 4 °C of heavy chain and β_2m for 2 h followed by dilution of the sample into 0.42 mM peptide solution, yielding the same final concentrations as above (2).

β_2m dissociation from the heterodimer as illustrated in Figure 8. At the first stage of the experiment (t_1), 20 μL of the heavy-chain stock solution (1.8 μM) was added to 140 μM of 0.1 μM β_2m−TR at 20 °C. The increase in emission intensity was due to the formation of the heavy chain/β_2m−TR heterodimer. Addition of excess β_2m at t_2 induced the exchange of the TR-labeled β_2m from the heterodimer. The dissociated β_2m−TR molecules oligomerized, which caused quenching of TR fluorescence as shown in the second part of the kinetic trace. Since oligomerization of β_2m−TR occurred faster than its dissociation from the heterodimer, the observed kinetics are mainly controlled by β_2m−TR dissociation from the heavy chain. The dissociation time course was biexponential with rate constants of (1.0 ± 0.2) × 10^{-2} s^{-1} and (9.8 ± 0.7) × 10^{-4} s^{-1} at 20 °C. It is noteworthy that the rate constants derived from the biexponential heterodimer dissociation quantitatively correlate with those calculated from the decay of the amplitude α_1 as shown in the inset to Figure 2. This correlation proves that the decline of the amplitude α_1 caused by the heterodimer dilution is indeed due to its dissociation.

Nonradiative energy transfer from the heavy-chain tryptophans to the dansyl chromophore (W ⟹ DNS) and a cascade of further transfer to TR attached to the β_2m (W ⟹ DNS ⟹ TR) was found to take place in the doubly labeled ternary complexes. The complex was produced by first mixing H-2K^b heavy chain with β_2m−TR (final concentrations were as in the previously described experiment), followed by addition of OVA7C-DNS peptide (0.5 μM final concentration). Peptide addition to the heavy chain preincubated with β_2m−TR further enhanced the intensity of the TR fluorescence, most probably due to the increase in affinity of β_2m and heavy chain, thereby increasing the number of the peptide complexes produced. The fluorescence signals D−F monitored at 530 nm (dansyl) upon excitation of tryptophans at 280 nm are proportional to the concentration of ternary complexes (Figure 9). Signals A−C monitored at 615 nm, where TR emits upon excitation at 280 nm, are

Table 3: Analysis of the Assembly Kinetics of H-2K^b Complex from Heavy Chain, β_2m, and OVA7C-DNS[a]

[β_2m] (μM)	α_1	τ_1 (s)	k_1 ($\times 10^4$ M^{-1} s^{-1})	α_2	τ_2 (s)	k_2 ($\times 10^{-3}$ s^{-1})
0.28	0.40 ± 0.05	44 ± 5	8.1 ± 1.0	0.60± 0.05	252 ± 50	4.0 ± 0.6
0.41	0.37± 0.05	29 ± 5	8.4 ± 1.0	0.63± 0.05	251 ± 50	4.0 ± 0.6
0.78	0.42± 0.05	18 ± 5	7.0 ± 1.0	0.58± 0.05	296 ± 50	3.4 ± 0.6

[a] Biexponential model: $y(t) = 1 - \alpha_1 \exp(-t/t_1) - \alpha_2 \exp(-t/t_2)$. t = 10 °C, [H-2K^b heavy chain] = 0.1 μM, [OVA7C-DNS] = 0.5 μM.

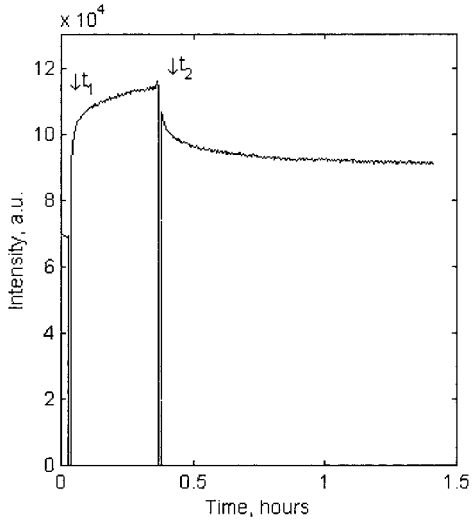

FIGURE 8: Assembly and dissociation time courses of H-2K^b heterodimer at 20 °C. The reaction was initiated by addition of 20 mL of H-2K^b heavy chain (1.6 μM) to 140 μL of TR-labeled C88S mutant β_2m solution (0.1 μM) at t_1; 20 μL of WT β_2m (6.3 μM) was added to the sample at t_2.

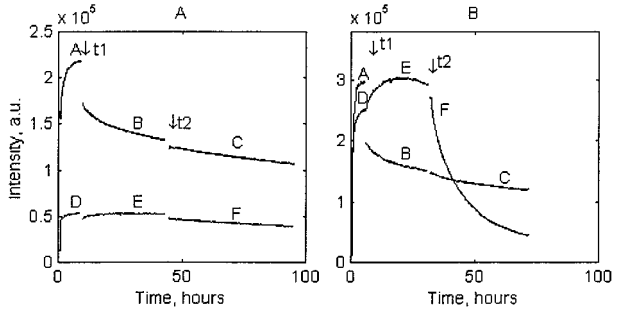

FIGURE 9: Time courses of peptide and β_2m dissociation from the H-2K^b/β_2m-TR/OVA7C-DNS (A) and H-2K^b/β_2m-TR/OVA3C-DNS doubly labeled ternary complex (20 °C). The ternary complex was produced by mixing of heavy chain, β_2m−TR, and OVA7C-DNS to final concentrations of 0.1, 0.08, and 0.5 μM respectively ($0 - t_1$ time domain). Exchange of the labeled for unlabeled β_2m was initiated by addition of unlabeled WT β_2m (2 μM final concentration) at t_1. OVA7C-DNS exchange was initiated by addition of OVA peptide (40 μM final concentration) at t_2. The 280/530 nm signals (D−F) represent concentration of the ternary complexes loaded with the dansylated peptide. The 280/615 nm signals (A−C) represent concentration of the doubly labeled complexes.

proportional to the concentration of the doubly labeled ternary complexes. Addition of a high concentration (2 μM) of unlabeled β_2m at t_1 started the exchange of labeled for unlabeled β_2m molecules, at a rate that was determined by β_2m−TR dissociation from the ternary complex. At the same time, addition of excess unlabeled β_2m also led to an increase in the total concentration of the ternary complexes since the concentration of the labeled β_2m−TR was chosen to be lower than that of heavy chains. Unlabeled OVA peptide (final concentration 40 μM) was then added to the sample at t_2. This enabled monitoring of OVA7C-DNS dissociation from the ternary complex via the dansyl group emission. The above experimental protocol allowed the independent comparison of both β_2m and peptide dissociation rates from the ternary complex under identical conditions. Parameters of a biexponential fit of the experimental decay curves B and F are summarized in Table 4. β_2m was found to dissociate from the ternary complex faster than OVA7C-DNS but slower than OVA3C-DNS.

Dissociation kinetics of OVA3C-DNS and OVA7C-DNS from the ternary K^b complex were found to be biexponential. A family of traces presenting the dissociation time course of OVA3C-DNS, the lowest affinity peptide of the studied series, from the ternary complex were recorded at 37 (1), 30 (2), 20 (3), 14 (4), and 10 °C (5) and are shown in the inset to Figure 10. Results of their biexponential analysis are summarized in Table 5. The peptide dissociation rate constants calculated from the time constants of the most stable fractions are plotted in the Arrhenius coordinates (Figure 10). For comparison, similar Arrhenius plots of peptide dissociation rate constants of the highest and lowest affinity peptides (dNP21 and dNP20) for H-2K^d/β_2m heterodimer are also plotted in this figure. Clearly, the dissociation rate constants of the highest affinity peptide (dNP20) from the K^d ternary complex are similar to those of the dissociation of the lowest affinity peptide OVA3C-DNS from the K^b ternary complex. As expected, peptide dissociation rate constants from the H-2K^b "free" heavy chain ($\triangledown$) are faster than from the ternary complex ($\triangle$) (as illustrated for OVA7C-DNS).

DISCUSSION

Scheme 1 describes the two distinct pathways through which the *in vitro* assembly of the ternary complex may proceed. This scheme is similar but differs in several crucial elements from that published earlier by Otten et al. (*36*). One pathway starts by association of the "free" heavy chain with β_2m (steps B and C) while the other begins with peptide binding to the heavy chain (step G). The rate constant of heavy-chain association with β_2m has now been determined to be much faster than that with peptides. The former is a composite process involving an intermediate step where the heavy chain conformer hc* is formed and binds to β_2m with a rate constant of about (8.0 ± 1.0) $\times$ 10^4 M^{-1} s^{-1} (10 °C), i.e., more than 2 orders of magnitude faster than that of peptide binding to the heavy chain (140 ± 30 M^{-1} s^{-1}). This suggests that hc* binding to β_2m does not involve further significant conformational changes. In contrast, the conformational transition hc $\Rightarrow$ hc* (step B) is a relatively slow process, therefore becoming a rate-limiting step in the ternary complex assembly. One of the heterodimer conformers, (hc*·β_2m)$_{act}$, binds peptides (step E) at (1.4 ± 0.4) $\times$ 10^5 M^{-1} s^{-1} (10 °C), i.e., about 2-fold faster than hc* binds to β_2m. Thus, the assembly rate of the H-2K^b ternary complex

Table 4: Analysis of the Dissociation Kinetic Curves of Doubly Labeled H-2K^b/β_2m−TR Complex Loaded with OVA3C-DNS or OVA7C-DNS[a]

	α_1	k_1 (s^{-1})	α_2	k_2 (s^{-1})
		H-2K^b/β_2m−TR/OVA3C-DNS		
peptide dissociation[b]	0.85 ± 0.10	$(2.5 \pm 1.0) \times 10^{-5}$	0.15 ± 0.10	$(2.1 \pm 0.6) \times 10^{-4}$
β_2m−TR dissociation[c]	0.74 ± 0.10	$(8.1 \pm 4.0) \times 10^{-6}$	0.26 ± 0.10	$(7.9 \pm 4.0) \times 10^{-5}$
		H-2K^b/β_2m-TR/OVA7C-DNS		
peptide dissociation[b]	$0.97 \pm {}^{0.03}_{0.10}$	$(3.1 \pm 1.0) \times 10^{-6}$	$0.03 \pm {}^{0.10}_{0.03}$	$(5.1 \pm 4.0) \times 10^{-4}$
β_2m−TR dissociation[c]	0.80 ± 0.10	$(7.5 \pm 2.0) \times 10^{-6}$	0.20 ± 0.10	$(7.6 \pm 2.0) \times 10^{-5}$

[a] $t = 19$ °C, [H-2K^b heavy chain] = 0.1 μM, [β_2m−TR] = 0.08 μM, [peptide] = 0.5 μM. [b] Curve F in Figure 9. [c] Curve B in Figure 9.

Table 5: Analysis of OVA3C-DNS Dissociation Kinetics from the H-2K^b Ternary Complex by Biexponential Model

t (°C)	α_1	k_1 (s^{-1})	α_2	k_2 (s^{-1})
10	1.00	$(1.7 \pm 0.4) \times 10^{-5}$	−	−
14	$0.94 \pm {}^{0.06}_{0.10}$	$(2.5 \pm 0.4) \times 10^{-5}$	$0.06 \pm {}^{0.10}_{0.06}$	$(4.4 \pm 1.0) \times 10^{-4}$
20	0.83 ± 0.10	$(3.3 \pm 0.5) \times 10^{-5}$	0.17 ± 0.10	$(3.0 \pm 1.0) \times 10^{-4}$
30	0.87 ± 0.10	$(2.5 \pm 0.4) \times 10^{-4}$	0.13 ± 0.10	$(2.1 \pm 0.8) \times 10^{-3}$
37	0.19 ± 0.10	$(1.0 \pm 0.2) \times 10^{-3}$	0.81 ± 0.10	$(6.9 \pm 1.0) \times 10^{-3}$

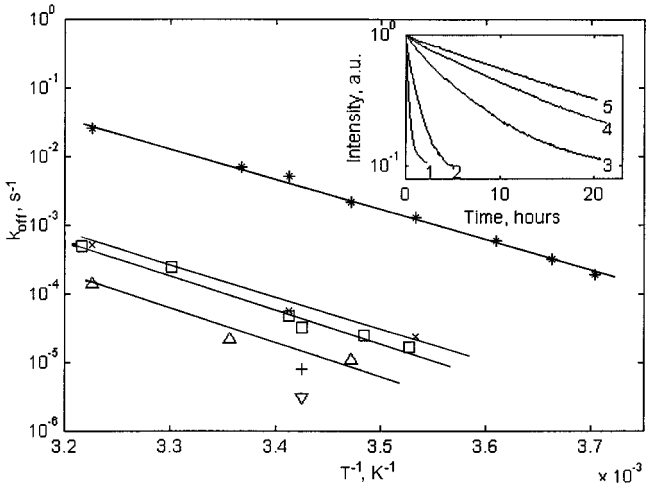

FIGURE 10: Arrhenius plots of peptide dissociation rate constants. Dissociation of (1) OVA3C-DNS from H-2K^b ternary complex (□); (2) OVA7C-DNS from H-2K^b heavy chain (△); (3) OVA7C-DNS from H-2K^b ternary complex (▽); (4) β_2m−TR from H-2K^b ternary complex loaded with OVA3C-DNS or OVA7C-DNS (+); and (5) dNP20 (×) and dNP21 (*) from H-2K^d ternary complex for comparison. (Inset) Time courses of OVA7C-DNS dissociation from H-2K^b ternary complex recorded at 37 (1), 30 (2), 20 (3), 14 (4), and 10 °C (5). The reactions were initiated by addition of excess (20 mM) unlabeled OVA peptide to 0.1 mM solution of H-2K^b/β_2m/OVA3C-DNS ternary complex.

strongly depends on the type of species present at the process initiation. For example, starting with separated components, the hc* will react with β_2m (step C) followed by peptide binding (steps D and E), where hc ⇒ hc* (step B) will be the rate-limiting step. In contrast, the assembly rate will be much faster if the heavy chain and β_2m have associated prior to peptide addition.

The amplitudes of the biexponential time course of complex assembly from heavy chain, β_2m, and peptide ($\alpha_1 \approx 0.4$ and $\alpha_2 \approx 0.6$; Table 3) suggest that the rate constant of the backward reaction (hc ⇐ hc*) is higher than that of the forward one. Thus, about 40% of the heavy chains existed in the hc* conformation at the start of the experiment. As the separated heavy chains tend to oligomerize in the absence of β_2m, the steady-state hc ⇔ hc* constantly shifts to the left, producing oligomers. This situation is reversed upon addition of β_2m at sufficiently high concentration. Namely, since hc* binding to β_2m will be faster than the heterodimer dissociation, hc oligomerization will be blocked. Oligomerization of newly synthesized heavy chains in the endoplasmic reticulum would obviously impede the ternary complex expression on the cells and therefore chaperones (e.g., calnexin) most likely assist the heavy chain's transformation into a conformation appropriate for association with β_2m (*37*).

Scheme 1

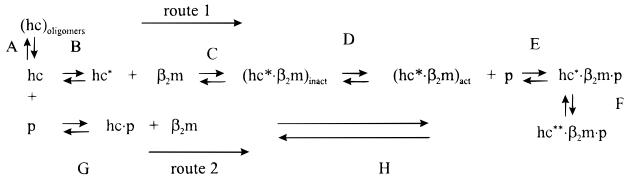

The biphasic time course of peptide binding to the heterodimer and its independence on the addition of excess β_2m clearly suggest that the heterodimers exist in two conformations, one of which does not bind peptides. The conversion of the inactive to the active conformation constitutes the rate-limiting step in the peptide binding to the heterodimer. The biexponential dissociation of the heavy chain/β_2m heterodimer is also consistent with the existence of these two conformations. The observation of nearly equal concentrations of the active and inactive heterodimers suggests that the rates of the forward and backward reactions (step D) are about equal. At 37 °C the first conformer binds peptides with a rate constant of $\sim 3.0 \times 10^6$ M^{-1} s^{-1}, which is very similar to rate constants of oligopeptide or oligosacharide binding to specific sites of antibodies or receptors (*38*). These are still about 2 orders of magnitude lower than those observed for smaller, rigid ligands (e.g., nitroaromatic haptens), which bind with rate constants in the range of 10^8 M^{-1} s^{-1} (*38*). This difference probably reflects the limits set on the final binding step of a floppy peptide where adjustments of both its own conformation as well as the MHC groove are required. Peptide binding to the heterodimer changes the conformation of the heavy chain hc* to hc** so that β_2m dissociation from hc** becomes much slower than from hc*. These results suggest that stability of the heavy chain/β_2m heterodimer significantly increases upon peptide

binding, apparently as result of the hc* ⇒ hc** conformational transition in the heavy chain. Therefore, it is possible that the peptide-induced heavy chain conformational transition not only stabilizes the heterodimer but also causes its dissociation from one of the peptide transporting proteins (TAP1), with which it associates in the "empty" state (*37*). Upon its release from TAP1, the ternary complex is in its most stable conformation, ready to be transported to the cell surface.

The alternative assembly route operating in vitro starts by peptide binding to "free" heavy chain (step G) and is followed by association with β_2m (step H). However, this pathway plays a minor role since the rate constant of peptide binding to the heavy chain is more than 100-fold slower than that of β_2m binding.

Stability of the H-2K^b ternary complex with the OVA peptide series is much greater than that of its H-2K^d counterpart with peptides of the NP series (*1*). This is apparently due to the fact that the employed K^d binding motif X**Y**X*X*XXXX**I**(**V,T,N,L**) has one anchor-side chain less than the K^b motif X**I(G,P)***I*X**F(Y)**XX**L** (*2*). The additional anchor-side chain interaction is apparently causing the formation of a relatively more stable complex between the "free" K^b heavy chain and OVA3C-DNS or OVA7C-DNS. Still, the significant affinity reduction for OVA3C-DNS compared with OVA7C-DNS indicates an important contribution of the $N + 3$ side chain to the peptide binding energy (*28*). A similar effect of the $N + 4$ side chain was also observed for peptide binding to the H-2K^d heterodimer; affinity of the NP peptide T**Y**Q*R*TRAL**V** was reduced by about 2 orders of magnitude when the fourth amino acid (arginine) was changed to cysteine (*1*).

Dissociation of β_2m from K^d ternary complexes was always slower than that of any peptides of the NP series. In contrast, β_2m was found to dissociate faster from K^b ternary complexes than certain peptides. As shown for the K^d ternary complexes, peptide dissociation reduces the heavy chain affinity for β_2m and leads to heterodimer dissociation, which in turn brings about the decay of the peptide binding conformation of the heavy chain. Since physiological fluids' β_2m concentrations are rather low, the reassembly of these ternary complexes on the cell surface from the "free" heavy chain, external β_2m, and exogenous peptide becomes inefficient. In addition to the above decay route, dissociation of K^b ternary complexes can also start from β_2m dissociation. When this takes place at the cell surface, the heavy chain/peptide complex may apparently persist for some time. This raises the interesting question to what extent the hc−peptide recognition by TCR may still take place. Despite the differences compared with K^d, the K^b heavy chains may also avoid binding of the exogenous peptides at the cell surface if upon dissociation of an endogenous peptide the conformation of the peptide binding groove quickly decays.

It is noteworthy that the binding rate constants of OVA3C-DNS and OVA7C-DNS to the K^b heterodimer have, within the limits of experimental accuracy, the same values. Moreover, these constants are essentially the same as those observed for peptides of the influenza virus nucleoprotein series binding to H-2K^d heterodimer. Thus, very similar rate constants were observed for binding of seven different nona- or octapeptides to two different MHC alleles. These findings apparently reflect universal characteristics of peptide association with the class I heterodimers and are indeed similar to the binding rate constants of floppy haptens to sites of specific monoclonal antibodies (*38*). Since all examined peptides bind the heterodimer with very similar rate constants, their affinities are determined by other steps in their complex assembly equilibrium (Scheme 1): Their dissociation rate constants are in the range from 2×10^{-6} to 5×10^{-4} s^{-1} (20 °C) for the highest and lowest affinity peptides, respectively. This implies that the affinities of the peptide−heavy chain/β_2m heterodimer interaction may be in the 10^{-11}−10^{-9} M range, i.e., similar to those of antigens with high-affinity antibodies. However, as expected for the complex equilibrium, considerable deviations are observed between binding constants determined by peptide equilibrium titrations and the k_{off}/k_{on} ratios calculated with the assumption that a single step describes the interaction equilibrium. Due to the lability of the heterodimer, the ternary complex assembly proceeds either via direct peptide binding to the heterodimer or via peptide binding to the hc** followed by β_2m binding. As shown here, these two processes have very different reaction rates. Although the heterodimer binds peptides with relatively fast rate constants, the assembly reaction may be significantly slower depending on actual concentrations of the reagents at the moment of the reaction initiation.

Results of the experiments presented here are consistent with those where kinetics of MHC-I molecules binding to synthetic peptides were done by surface plasmon resonance (*27*, *28*, *39*, *40*). The advantage of the currently employed experimental approach lies in the unambiguous assignment of the molecular steps. i.e., monitoring directly the specific peptide or β_2m binding steps. This is due to the resonance fluorescence energy transfer process, which takes place from groove-proximal tryptophan residues to the DNS conjugated to the bound peptide and further to the TR conjugated to β_2m, or due to fluorescence intensity changes of the TR-derivatized β_2m, processes which are highly sensitive to proximity between the two reaction partners. In contrast, plasmon resonance measures changes in the refractive index near the substrate-immobilized peptides upon the heterodimer binding. These interactions take place at the gel/solution interface, which makes them susceptible to a variety of complications related to accessibility and diffusion. Nevertheless, it is gratifying that the apparent K_d values obtained for the interaction between various derivatized analogues of the OVA peptide 257−264 and H-2K^b by both methods are in good agreement.

In summary, we conclude that H-2K^b and H-2K^d share common features in their ternary complex assembly processes, though some quantitative differences exist between their dissociation mechanisms: (1) heavy chain/β_2m heterodimers of both alleles bind peptides with very similar rate constants; (2) the "free" heavy chains either do not bind or bind peptides about 3 orders of magnitude more slowly than their heterodimers; (3) the rate-limiting step in the ternary complex assembly of both alleles is determined by the hc ⇒ hc* transition; and (4) the heterodimers are relatively short-lived with half-lives of minutes at physiological temperature yet achieve significant stabilization upon peptide binding. All of these features are the result of the allosteric interactions among the heavy chain, β_2m, and peptides, which

may turn out to take place for all alleles of class I MHC molecules.

ACKNOWLEDGMENT

We thank Dr. Alexander Goldin (agoldin@netvision.net.il) for providing the program for global least-squares analysis.

REFERENCES

1. Gakamsky, D. M., Bjorkman, P. J., and Pecht, I. (1996) *Biochemistry 35*, 14841−14848.
2. Engelhard, V. H. (1994) *Annu. Rev. Immunol. 12*, 181−207.
3. Rammensee, H. G. (1996) *Int. Arch. Allergy Immunol. 110*, 299−307.
4. Rock, K. L., Gamble, S., Rothstein, L., Gramm, C., and Benacerraf, B. (1991) *Cell 65*, 611−620.
5. Parker, K. C., DiBrino, M., Hull, L., and Coligan, J. E. (1992) *J. Immunol. 149*, 1896−1904.
6. Matsumura, M., Saito, Y., Jackson, M. R., Song, E. S., and Peterson, P. A. (1992) *J. Biol. Chem. 267*, 23589−23595.
7. Horig, H., Papadopoulos, N. J., Vegh, Z., Palmieri, E., Angeletti, R. H., and Nathenson, S. G. (1997) *Proc. Natl. Acad. Sci. U.S.A. 94*, 13826−13831.
8. Morgan, C. L., Ruprai, A. K., Solache, A., Lowdell, M., Price, C. P., Cohen, S. B., Parham, P., Madrigal, J. A., and Newman, D. J. (1998) *Immunogenetics 48*, 98−107.
9. Springer, S., Doring, K., Skipper, J. C., Townsend, A. R., and Cerundolo, V. (1998) *Biochemistry 37*, 3001−3012.
10. Kozlowski, S., Takeshita, T., Boehncke, W. H., Takahashi, H., Boyd, L. F., Germain, R. N., Berzofsky, J. A., and Margulies, D. H. (1991) *Nature 349*, 74−77.
11. Otten, G. R., Bikoff, E., Ribaudo, R. K., Kozlowski, S., Margulies, D. H., and Germain, R. N. (1992) *J. Immunol. 148*, 3723−3732.
12. Ribaudo, R. K., and Margulies, D. H. (1992) *J. Immunol. 149*, 2935−2944.
13. Solheim, J. C., Cook, J. R., and Hansen, T. H. (1995) *Immunol. Res. 14*, 200−217.
14. Solheim, J. C., Harris, M. R., Kindle, C. S., and Hansen, T. H. (1997) *J. Immunol. 158*, 2236−2241.
15. Bouvier, M. and Wiley, D. C. (1998) *Nat. Struct. Biol. 5*, 377−384.
16. Shields, M. J., Kubota, R., Hodgson, W., Jacobson, S., Biddison, W. E., and Ribaudo, R. K. (1998) *J. Biol. Chem. 273*, 28010−28018.
17. Shields, M. J., Moffat, L. E., and Ribaudo, R. K. (1998) *Mol. Immunol. 35*, 919−928.
18. Catipovic, B., Talluri, G., Oh, J., Wei, T., Su, X. M., Johansen, T. E., Edidin, M., and Schneck, J. P. (1994) *J. Exp. Med. 180*, 1753−1761.
19. Sherman, L. A., Chattopadhyay, S., Biggs, J. A., Dick, R. F. d., and Bluestone, J. A. (1993) *Proc. Natl. Acad. Sci. U.S.A. 90*, 6949−6951.
20. Lie, W. R., Myers, N. B., Gorka, J., Rubocki, R. J., Connolly, J. M., and Hansen, T. H. (1990) *Nature 344*, 439−441.
21. Lie, W. R., Myers, N. B., Connolly, J. M., Gorka, J., Lee, D. R., and Hansen, T. H. (1991) *J. Exp. Med. 173*, 449−459.
22. Haugland, R. P. (1996) *Handbook of fluorescence probes and research chemicals*, 6th ed., p 679, Molecular Probes, Eugene, OR.
23. Davis, D. M., Reyburn, H. T., Pazmany, L., Chiu, I., Mandelboim, O., and Strominger, J. L. (1997) *Eur. J. Immunol. 27*, 2714−2719.
24. Wetlaufer, D. B. (1962) *Adv. Protein Chem. 17*, 303−390.
25. Parker, C. A. (1968) *Photoluminescence of solutions*, Elsevier, Amsterdam.
26. Rotzschke, O., Falk, K., Stevanovic, S., Gnau, V., Jung, G., and Rammensee, H. G. (1994) *Immunogenetics 39*, 74−77.
27. Khilko, S. N., Corr, M., Boyd, L. F., Lees, A., Inman, J. K., and Margulies, D. H. (1993) *J. Biol. Chem. 268*, 15425−15434.
28. Khilko, S. N., Jelonek, M. T., Corr, M., Boyd, L. F., Bothwell, A. L., and Margulies, D. H. (1995) *J. Immunol. Methods 183*, 77−94.
29. Schneck, J., Maloy, W. L., Coligan, J. E., and Margulies, D. H. (1989) *Cell 56*, 47−55.
30. Hochman, J. H., Shimizu, Y., DeMars, R., and Edidin, M. (1988) *J. Immunol. 140*, 2322−2329.
31. Fremont, D. H., Matsumura, M., Stura, E. A., Peterson, P. A., and Wilson, I. A. (1992) *Science 257*, 919−927.
32. Fremont, D. H., Stura, E. A., Matsumura, M., Peterson, P. A., and Wilson, I. A. (1995) *Proc. Natl. Acad. Sci. U.S.A. 92*, 2479−2483.
33. Matsumura, M., Fremont, D. H., Peterson, P. A., and Wilson, I. A. (1992) *Science 257*, 927−934.
34. Zhang, W., Young, A. C., Imarai, M., Nathenson, S. G., and Sacchettini, J. C. (1992) *Proc. Natl. Acad. Sci. U.S.A. 89*, 8403−8407.
35. Gakamsky, D. M., Davis, D. M., Haas, E., Strominger, J. L., and Pecht, I. (1999) *Biophys. J. 76*, 1552−1560.
36. Otten, G. R., Bikoff, E., Ribaudo, R. K., Kozlowski, S., Margulies, D. H., and Germain, R. N. (1992) *J. Immunol. 148*, 3723−3732.
37. Vassilakos, A., Cohen-Doyle, M. F., Peterson, P. A., Jackson, M. R., and Williams, D. B. (1996) *EMBO J. 15*, 1495−1506.
38. Pecht, I., and Lancet, D. (1977) in *Chemical relaxation in molecular biology* (Pecht, I., and Rigler, R., Eds.) pp 306−336, Springer-Verlag, Berlin, Heidelberg, and New York.
39. Margulies, D. H., Corr, M., Boyd, L. F., and Khilko, S. N. (1993) *J. Mol. Recognit. 6*, 59−69.
40. Margulies, D. H., Plaksin, D., Khilko, S. N., and Jelonek, M. T. (1996) *Curr. Opin. Immunol. 8*, 262−270.

BI9905821